Acta Crystallographica Section D
Biological Crystallography
ISSN 0907-4449

Crystallization of the *Mycobacterium tuberculosis* cell-division protein FtsZ

Adelaine K. W. Leung, E. Lucile White, Larry J. Ross and David W. Borhani*†

Drug Discovery Division, Southern Research Institute, Birmingham, AL 35205, USA

† Present address: BASF Bioresearch Corp., 100 Research Drive, Worcester, MA 01605, USA.

Correspondence e-mail: borhand@basf.com

Received 14 June 2000
Accepted 29 August 2000

Mycobacterium tuberculosis FtsZ (MtbFtsZ), an essential protein in bacterial cell division, has been crystallized in the presence of a new inhibitor of MtbFtsZ polymerization and GTPase activity, ethyl (6-amino-2,3-dihydro-4-phenyl-1*H*-pyrido[4,3-*b*][1,4]diazepin-8-yl)-carbamate (SRI-7614). Crystals of the MtbFtsZ–SRI-7614 complex (form I, 30% polyethylene glycol 4000, 0.1 *M* sodium citrate pH 5.6, 0.2 *M* NH_4OAc, 293 K) belong to space group $P6_1$ or $P6_5$, with unit-cell parameters a = 88.78, c = 178.02 Å, and diffract to 2.3 Å resolution. A second crystal form, of the GDP complex, grows in the presence or absence of Mg^{2+} from PEG 4000 at 277 K or from $(NH_4)_2SO_4$ at 293 K, respectively (form II, space group $P6_222$ or $P6_422$, with unit-cell parameters a = 135.02, c = 328.97 Å or a = 129.30, c = 327.97 Å, respectively). Complete data sets to ∼7 Å resolution have been collected from both. Exceptional form II crystals diffract to at least 4.5 Å resolution. Determination of the MtbFtsZ structure may advance the design of improved inhibitors of FtsZ polymerization.

1. Introduction

Tuberculosis (TB), which is caused by *M. tuberculosis*, is the second leading cause of infectious disease death in the world, claiming nearly three million lives each year. TB is increasingly prevalent in AIDS patients since HIV infection greatly increases the risk of a latent infection developing into active disease (National Action Plan to Combat Multidrug-Resistant Tuberculosis, 1992). The difficulty and sometimes outright failure of existing TB treatments, the association with HIV infection and the recent alarming emergence of multi-drug-resistant *M. tuberculosis* strains have all spurred the search for new drugs to treat TB.

FtsZ (from filamenting temperature-sensitive strain Z) is a ubiquitous 40 kDa protein in eubacteria and archaea that is an ortholog of eukaryotic tubulin (Lutkenhaus & Addinall, 1997; Erickson *et al.*, 1996; Erickson, 2000). During bacterial cell division FtsZ polymerizes in a GTP-dependent manner to form the 'Z-ring' structure located on the inner surface of the cellular membrane. Contraction of the Z ring, orchestrated with other *fts* gene products (*e.g.* FtsA; Yan *et al.*, 2000), leads to invagination, septum formation and daughter-cell separation. The only FtsZ atomic structure known is that from *Methanococcus jannaschii* (Löwe & Amos, 1998). The structure revealed that FtsZ and mammalian tubulin are structurally analogous (Nogales, Wolf *et al.*, 1998) and that together they form a novel GTPase family (Nogales, Downing *et al.*, 1998).

FtsZ is a novel target for drug design since it is essential for cell division in mycobacteria. Recent work at Southern Research Institute has identified a poor inhibitor of mammalian tubulin polymerization, ethyl (6-amino-2,3-dihydro-4-phenyl-1*H*-pyrido[4,3-*b*][1,4]diazepin-8-yl)carbamate (SRI-7614; Temple & Rener, 1992), that also inhibits *M. tuberculosis* FtsZ (MtbFtsZ) polymerization and GTPase activity (White *et al.*, 2000). We have crystallized MtbFtsZ in the presence of either SRI-7614 or GDP. The MtbFtsZ–SRI-7614 complex crystals, which diffract X-rays to 2.3 Å resolution, are amenable to structure determination.

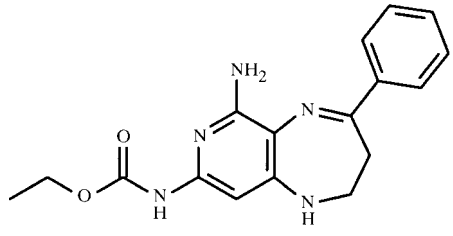

SRI-7614

2. Results

2.1. Crystallization in the presence of SRI-7614

Recombinant MtbFtsZ, comprising residues 1–379 plus an N-terminal Gly-Ser-His peptide remnant of the pET15b vector, was purified as described by White *et al.* (2000). MtbFtsZ (10–20 mg ml^{-1} in 25 m*M* Na HEPES pH 7.2,

© 2000 International Union of Crystallography
Printed in Denmark – all rights reserved

Table 1
Data statistics for *M. tuberculosis* FtsZ crystals.

Crystal form	I	II	II
Ligand	SRI-7614	GDP	Mg^{2+}-GDP
Data-collection site	Laboratory	NSLS X25	SSRL 9-1
Wavelength (Å)	1.54	1.10	0.785
Space group	$P6_1$ or $P6_5$	$P6_222$ or $P6_422$	$P6_422$
a (Å)	88.78	129.30	135.02
c (Å)	178.02	327.97	328.97
Resolution range (Å)	15.0–2.30	30.0–6.85	26.8–7.38
No. of observations	181527	49526	8294
No. of unique reflections	35126	3061	2550
Mosaicity (°)	0.5	0.5	0.8
Overall			
R_{sym} (%)	9.5	7.1	7.0
$I/\sigma(I)$	10.5	26.7	10.8
Data completeness (%)	99.7	98.7	96.1
Mean multiplicity	5.2	16.2	3.3
Highest shell			
Resolution range (Å)	2.36–2.30	7.27–6.85	7.83–7.38
R_{sym} (%)	48.7	30.6	25.9
$I/\sigma(I)$	2.4	7.9	4.2
Data completeness (%)	100.0	99.4	98.3
Mean multiplicity	4.3	11.2	3.4

0.1 m*M* EDTA, 10 m*M* DTT, 3 m*M* NaN_3, 10% glycerol) was used for initial crystallization trials. Sparse-matrix screening (vapor diffusion at 277 and 293 K, 1:1 protein:well ratio; Crystal Screen Kits, Hampton Research; Jancarik & Kim, 1991; Carter & Carter, 1979) of MtbFtsZ in the presence of 2 m*M* SRI-7614 identified one crystallization condition (30% PEG 4000, 0.1 *M* sodium citrate pH 5.6, 0.2 *M* NH_4OAc, 293 K). These form I crystals were pointed rods (0.3 × 0.1 × 0.1 mm; Fig. 1*a*). Crystals were prepared for data collection by soaking in mother liquor containing 15% glycerol followed by flash-cooling in liquid nitrogen. X-ray diffraction data were collected at 100 K from a form I crystal in our laboratory by the rotation method (0.25° frames, 1800 s; Siemens Cu $K\alpha$ rotating anode, 50 kV, 108 mA; MAR Research image plate with Osmic optics; see Fig. 2*a*). Data were processed with *MOSFLM* (Leslie, 1992), *SCALA* (Evans, 1997) and *TRUNCATE* (French & Wilson, 1978). Additional processing was performed with the *CCP*4 package (Collaborative Computational Project, Number 4, 1994). Integration of these data in Laue class 6/*m* with unit-cell parameters a = 88.78, c = 178.02 Å provided a complete 2.3 Å data set (Table 1). Examination of the [00*l*] reflections demonstrated that reflections with indices $l \neq 6n$ were absent, thus indicating the space group to be either $P6_1$ or $P6_5$. For the form I unit cell, one MtbFtsZ molecule per asymmetric unit gives a solvent content of 77% (Matthews coefficient V_M = 5.19 Å^3 Da^{-1}; Matthews, 1968), values that are unlikely given the strong diffraction exhibited by these crystals. Two molecules in the asymmetric unit gives a solvent content of 53% and a V_M of 2.59 Å^3 Da^{-1}. The self-rotation function was consistent with these latter values and showed the presence of a non-crystallographic twofold axis slightly misaligned (∼1°) with the a axis, *i.e.* the space group is pseudo-$P6_{1(5)}22$. That $P6_{1(5)}22$ is not the true space group was demonstrated by the significantly poorer scaling ($R_{sym} \simeq 20\%$) in $P6_{1(5)}22$ compared with $P6_{1(5)}$ (Table 1).

Molecular replacement structure determination of the MtbFtsZ–SRI-7614 complex, using the structure of *M. jannaschii* FtsZ as the search model, is under way. Initial calculations have not been promising, perhaps as a consequence of the low level of sequence similarity (57%). Therefore, we are also pursuing a heavy-atom based phasing strategy. Determination of this structure, which to our knowledge will be the first in the presence of an FtsZ polymerization inhibitor, will allow us to begin a structure-assisted drug-design program.

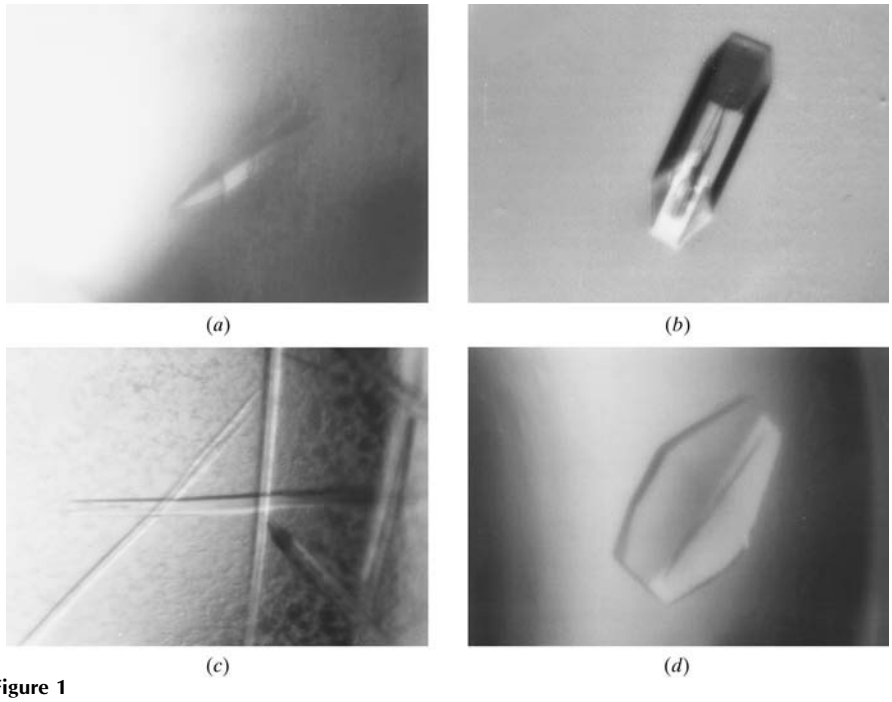

Figure 1
Crystals of *M. tuberculosis* FtsZ. (*a*) Form I crystal of the MtbFtsZ–SRI-7614 complex grown from 30% PEG 4000, 0.1 *M* sodium citrate pH 5.6, 0.2 *M* NH_4OAc at 293 K. (*b*) Form II crystal (0.4 × 0.1 × 0.1 mm) of the MtbFtsZ–Mg^{2+}-GDP complex grown from 28% PEG 4000, 0.1 *M* Tris–HCl pH 8.7, 0.2 *M* Li_2SO_4 at 277 K. Similar crystals also grew when GDP was replaced by the GTP analog 5′-guanyl-imidodiphosphate (GDPNP, Sigma G-0635; 2 m*M*). (*c*) Crystals (>1 × 0.1 × 0.1 mm) of the MtbFtsZ–Mg^{2+}-GDP complex grown from 10% 2-propanol, 20% PEG 4000, 0.1 *M* Na HEPES pH 7.5 at 293 K. (*d*) Form II crystal of the MtbFtsZ–GDP complex (no Mg^{2+}) grown from 1.4 *M* $(NH_4)_2SO_4$, 0.5 *M* NaCl, 0.1 *M* Na HEPES pH 7.2 at 293 K.

2.2. Crystallization in the presence of nucleotides

Since FtsZ polymerization depends on the binding and hydrolysis of guanine nucleotides, it was of interest to examine crystallization of MtbFtsZ in the presence of GDP and GTP analogues. Sparse-matrix screening of the MtbFtsZ–GDP complex in the presence of $MgCl_2$ identified more than ten crystallization conditions, comprising three major types, all near neutral pH. Crystals grew in the presence of 10 m*M* $MgCl_2$ and 2 m*M* GDP within 1 d from polyethyleneglycol with or without added salts (crystal form II; Fig. 1*b*), $(NH_4)_2SO_4$ and other salts, and PEG/alcohol mixtures (Fig. 1*c*). Although many of these crystals had sharp edges and were birefringent, none of them diffracted X-rays in the laboratory at either 100 K or mounted in capillaries at 277 K, even though very long exposures (0.2° rotation, 1 h) were used. The reasons for this lack of diffraction are not clear.

Because the oligomeric distribution of the *Escherichia coli* FtsZ–GDP complex is modulated by the presence or absence of Mg^{2+} (Sossong *et al.*, 1999), being predominantly monomeric in the absence of Mg^{2+},

we crystallized MtbFtsZ in the presence of 2 m*M* GDP but without $MgCl_2$ (10 m*M* EDTA included to chelate adventitious Mg^{2+}). Crystals grew under the above conditions as well as from 1.4–1.8 *M* $(NH_4)_2SO_4$, 0.5 *M* NaCl, 0.1 *M* Na HEPES pH 7.2, 293 K (multifaceted hexagonal blocks or plates, 0.4 × 0.4 × 0.1 mm; Fig. 1*d*). Substitution of KCl for NaCl did not affect crystal growth, despite the fact that MtbFtsZ can be both polymerized and depolymerized in the presence of 0.1 *M* KCl, whereas polymerization only is observed in the presence of 0.1 *M* NaCl (White *et al.*, 2000).

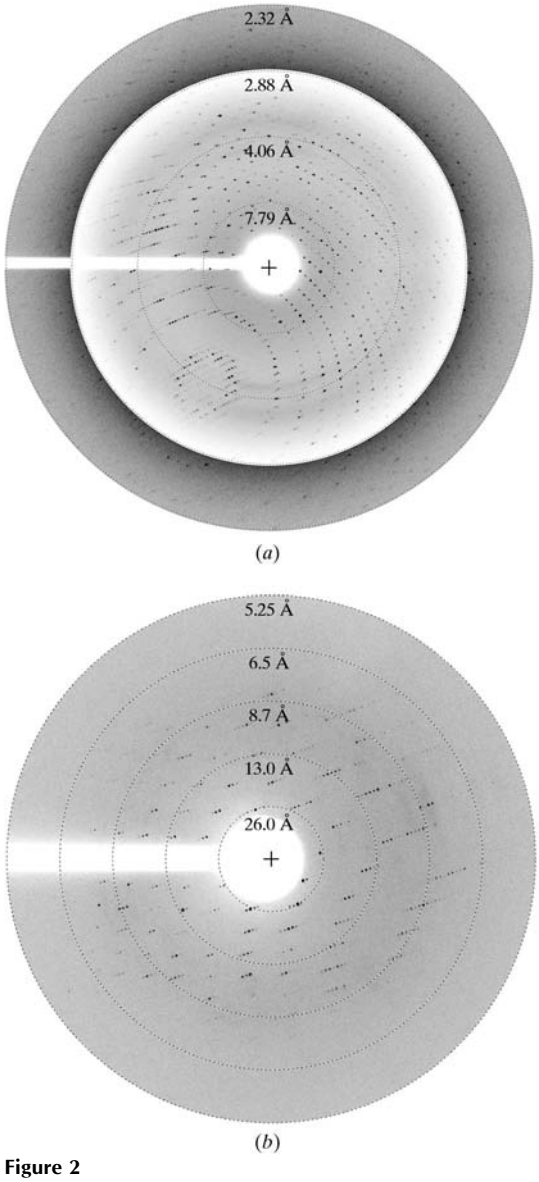

Figure 2
M. tuberculosis FtsZ X-ray diffraction patterns. (*a*) Diffraction pattern from a form I crystal (SRI-7614 complex; 0.25°, 1800 s, rotating anode) (Table 1; see Fig. 1*a*). The high-resolution diffraction data have been intensified to demonstrate the reflections at 2.3 Å resolution. (*b*) Diffraction pattern from a form II crystal (Mg^{2+}-free GDP complex; 1° rotation, 10 s, NSLS) (Table 1; see Fig. 1*d*). The crystal diffracts to 6.85 Å resolution.

A crystal grown under these new Mg^{2+}-free conditions diffracted weakly to 8 Å in the laboratory (100 K, 0.25°, 900 s), a definite improvement over the crystals grown in the presence of Mg^{2+}.

Diffraction data were collected from MtbFtsZ–GDP form II crystals at the National Synchrotron Light Source (Mg^{2+}-free; Brandeis B4 CCD detector; 1°, 10 s; see Fig. 2*b*) and the Stanford Synchrotron Radiation Laboratory (Mg^{2+}; MAR Research image-plate detector; 0.25°, 240 s). Integration of these data in Laue class 6/*mmm* with unit-cell parameters a = 129.30, c = 327.97 Å (Mg^{2+}-free) or a = 135.02, c = 328.97 Å (Mg^{2+}) provided 6.85 and 7.38 Å data sets, respectively (Table 1). Axial [00l] reflections with indices $l \neq 3n$ were absent in the Mg^{2+}-free data set, indicating the space group to be either $P6_222$ or $P6_422$. Although no axial reflections were recorded for the Mg^{2+} data set, the identical Laue symmetries and nearly identical unit-cell parameters suggest to us that both crystals adopt space group $P6_{2(4)}22$ and that both can be considered to be form II despite the very different crystallization conditions. Recently, a larger form II crystal (Mg^{2+}) diffracted to ∼4.5 Å resolution in the laboratory. We are hopeful that this crystal may diffract to higher resolution at the synchrotron (4.0–3.5 Å or better).

Self-rotation function calculations showed that the form II crystals possess a non-crystallographic twofold rotation axis located 15° away from the *a* axis in the *ab* plane. Thus, two (or more) MtbFtsZ subunits are present in the asymmetric unit. The presence of two molecules in the asymmetric unit (solvent content 76%; V_M = 5.07 Å^3 Da^{-1}) would be consistent with the poor diffraction characteristics of these crystals and the fact that MtbFtsZ appears to be predominantly a dimer in solution (White *et al.*, 2000).

3. Discussion

The natural tendency of FtsZ to assemble and disassemble during the cell-division cycle may bias the formation of certain crystal forms or molecular-packing arrangements. That MtbFtsZ–GDP crystallizes under very different conditions to provide essentially the same form II crystals could mean that the observed hexagonal symmetry and particular unit-cell parameters reflect an intrinsic structural preference of MtbFtsZ polymers. Electron-microscopic studies on MtbFtsZ reveal that it polymerizes to form strands (diameter 3.7 nm), which pair to form parallel protofilaments (diameter 7–10 nm; White *et al.*, 2000). Similar protofilaments were observed with *M. jannaschii* FtsZ (Löwe & Amos, 1999). The protofilament diameter is commensurate with the hexagonal *a* axial length (∼13 nm). Furthermore, *E. coli* FtsZ forms mini-rings (23 nm diameter) and open 4-start helical structures (23 nm diameter, pitch 18 or 24°) under certain conditions (Lu *et al.*, 2000). It is tempting to speculate therefore that the 6_2 (or 6_4) screw axis with a ∼33 nm repeat distance observed in the MtbFtsZ form II crystals reflects an underlying helical structure of the FtsZ polymer in the crystals. Thus, determination of the GDP complex structure, even at low resolution, may provide a packing model that can be related to the structural features possessed by MtbFtsZ in its natural polymerized state.

E. coli and *Thermotoga maritima* FtsZs tend to form protofilaments even under conditions that inhibit GTPase activity and polymerization (Lu *et al.*, 1998). While MtbFtsZ does not exhibit this tendency (White *et al.*, 2000), formation and lateral association of protofilaments may nonetheless be an early part of crystal growth and non-uniform protofilament association may decrease the resolution limit of MtbFtsZ crystals. Since SRI-7614 appears to inhibit MtbFtsZ polymerization by preventing the lateral association of protofilaments (White *et al.*, 2000), co-crystallization experiments of MtbFtsZ–SRI-7614 under all current conditions (including those with GDP) are under way to examine the effect on crystal quality.

We thank Alex Kuzin for assistance with the synchrotron data collection and Robert Reynolds and Lainne Seitz for supplying SRI-7614. We also thank Mike Soltis and Paul Ellis (Stanford Synchrotron Radiation Laboratory) and Bob Sweet (National Synchrotron Light Source). This work was supported by Southern Research Institute (Project No. 1045).

References

Carter, C. W. Jr & Carter, C. W. (1979). *J. Biol. Chem.* **254**, 12219–12223.

Collaborative Computational Project, Number 4 (1994). *Acta Cryst.* D**50**, 760–763.

Erickson, H. P. (2000). *J. Cell Biol.* **148**, 1103–1105.

Erickson, H. P., Taylor, D. W., Taylor, K. A. & Bramhill, D. (1996). *Proc. Natl Acad. Sci. USA*, **93**, 519–523.

Evans, P. R. (1997). *Jnt CCP4/ESF–EACBM Newslett. Protein Crystallogr.* **33**, 22–24.

French, S. & Wilson, K. (1978). *Acta Cryst.* A**34**, 517–525.

Jancarik, J. & Kim, S.-H. (1991). *J. Appl. Cryst.* **24**, 409–411.

Leslie, A. G. W. (1992). *Jnt CCP4/ESF–EACMB Newslett. Protein Crystallogr.* **26**.

Löwe, J. & Amos, L.A. (1998). *Nature (London)*, **391**, 203–206.

Löwe, J. & Amos, L. A. (1999). *EMBO J.* **18**, 2364–2371.

Lu, C., Reedy, M. & Erickson, H. P. (2000). *J. Bacteriol.* **182**, 164–170.

Lu, C., Stricker, J. & Erickson, H. P. (1998). *Cell Motil. Cytoskeleton*, **40**, 71–86.

Lutkenhaus, J. & Addinall, S. G. (1997). *Annu. Rev. Biochem.* **66**, 93–116.

Matthews, B. W. (1968). *J. Mol. Biol.* **33**, 491–497.

National Action Plan to Combat Multidrug-Resistant Tuberculosis (1992). *MMWR Morb. Mortal. Wkly Rep.* **41**, 1–71.

Nogales, E., Downing, K. H., Amos, L. A. & Löwe, J. (1998). *Nature Struct. Biol.* **5**, 451–458.

Nogales, E., Wolf, S. G. & Downing, K. H. (1998). *Nature (London)*, **391**, 199–203.

Sossong, T. M. Jr, Brigham-Burke, M. R., Hensley, P. & Pearce, K. H. (1999). *Biochemistry*, **38**, 14843–14850.

Temple, C. Jr & Rener, G. A. (1992). *J. Med. Chem.* **35**, 4809–4812.

White, E. L., Ross, L. J., Reynolds, R. C., Seitz, L. E., Moore, G. D. & Borhani, D. W. (2000). *J. Bacteriol.* **182**, 4028–4034.

Yan, K., Pearce, K. H. & Payne, D. J. (2000). *Biochem. Biophys. Res. Commun.* **270**, 387–392.